Chipless RFID-Based Sensing Under Varying Seedling Tray Density and Plant Water Content

Anil Tulu*, Mehmet Emre Korkmaz*, Qammer H. Abbasi†, Sema Dumanli*
*Bogazici University, Electrical Electronics Engineering, Istanbul, Turkiye, sema.dumanli@bogazici.edu.tr
†James Watt School of Engineering, University of Glasgow, Glasgow, UK, Qammer.Abbasi@glasgow.ac.uk

***Abstract*—The integration of Chipless Radio Frequency Identification sensors offers a sustainable solution to traditional Internet of Things sensors in agricultural technologies. This paper analyses the backscatter link robustness for a C-like tag designed for plant growth monitoring. The readability of the tag is investigated under two environmental variables, planting density and plant water content. The tag is located in a 40 cm by 40 cm seedling tray, while the effect of variables is analysed using the decrease in peak height of the calibrated transmission coefficient data. As planting density increases from 5 by 5 to 9 by 9, the peak height drops by at least 3 dB. This drop tends to grow with higher plant water content, although at a fixed density, the effect of water content is modest. The results are crucial for understanding the environmental effects on sensing in real-life scenarios.**

***Index Terms*—Chipless RFID, Plant-Growth Monitoring, Backscatter Communication, Agricultural Technologies, Biodegradable Sensors.**

I. Introduction

Advancements in wireless technologies lead to the development of new kinds of sensor devices that can monitor various environmental parameters like temperature, light, moisture, and CO_2 level. This capability of tracking parameters has significantly transformed precision agriculture on the road to maximizing crop yield and minimizing resource waste. Internet of Things (IoT) based sensors are mostly used in agricultural monitoring [1], but these IoT devices rely on bulky batteries and complex electronic circuits, which have high costs and end up as electronic waste.

To address the need for cost-effective and environmentally friendly solutions, Chipless Radio Frequency Identification (CRFID) sensors offer a strong alternative. CRFID tags are fully passive resonator structures, operating without the need for active electronics or internal power sources [2]. Many agricultural applications can be found in literature, such as ripeness monitoring [3], leaf wetness detection [4], gas detection and temperature monitoring [5]. Further using fully biodegradable materials like zinc as the conductor and Polylactic Acid (PLA) [6] or paper for substrate [7], these CRFID sensors can be environmentally friendly, and used in large-scale monitoring applications minimizing the carbon footprint.

Although these sensors offer many advantages, the operational range is a major challenge for CRFID sensors. The performance of these systems must be rigorously investigated in harsh environments. Particularly in a greenhouse, dense plantation and changing water content of the plants act as strong absorbers and scatterers of microwave energy. This channel loss can severely degrade the performance of the sensor, specifically reducing the depth of its spectral notch, which can make the sensor unreadable.

In this paper, the operational performance of a fully biodegradable, on-plant C-like CRFID sensor specifically designed for plant growth monitoring is investigated for two variables in a 40 cm $\times$ 40 cm seedling tray. The first scenario is varying planting density of 5 $\times$ 5, 7 $\times$ 7, and 9 $\times$ 9. The second scenario is changing the water content of the plant. The relative permittivity of the plant is assumed to be homogeneous and is varied using the values 30, 50, and 70. The C-like CRFID resonator detection procedure is detailed in Section II and the environmental effects are modelled in Section III. The simulation results are discussed in Section IV and the paper concludes in Section V.

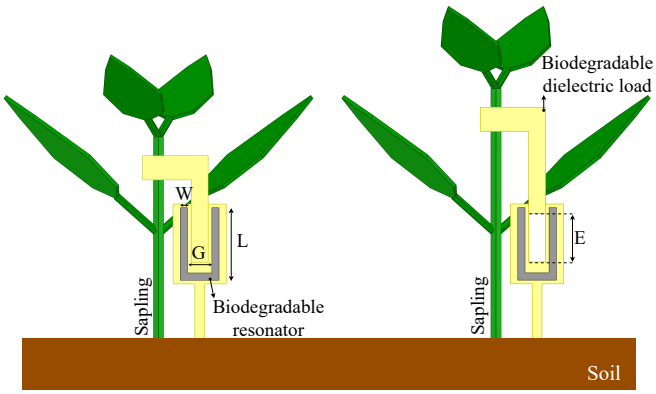

Fig. 1: Fully biodegradable C-like CRFID tag model: L = 15, G = 5, W = 1.5 mm, E = 0 to 10 mm. The dielectric load is attached to the trunk and freely slides inside the CRFID tag.

II. Chipless RFID Tag Detection

Sensing with CRFID tags depends on the change in resonant frequency as the medium parameters of the tag differ, and this change can be tracked with an antenna. Previously, the authors proposed a CRFID tag design and demonstrated how the growth monitoring mechanism [8]. Here, we focus on the readability of the tags. The tag that we used for this investigation is a C-like CRFID tag, as can be seen in Fig. 1.

To make the CRFID tag design environmentally friendly, the dielectric parts are chosen as PLA with a relative permittivity

978-88-31299-12-1/26/$31.00 ©2026 IEEE

of 2.5, and the conductive resonator is chosen as Zinc with a thickness of 50 μm, which are both biodegradable materials. The length of the arms (L) of the C-like structure is 15 mm, the width of the strips (W) is 1.5 mm, and the gap between the arms is 5 mm. This resonator structure is encapsulated with PLA, and a handle is added to the design to place into the soil. The dielectric load is designed so that it can freely slide between the arms of the encapsulated tag.

In this study, a reference-based calibration method is applied to eliminate the effects of the environment and to obtain the true reflection parameters of the CRFID tag [10]. This technique relies on using the response obtained using the Tag Under Test (TUT) containing the resonant structure ($S_{TUT} = Re[S_{TUT}] + Im[S_{TUT}]$) and a corresponding reference measurement ($S_{ref} = Re[S_{ref}] + Im[S_{ref}]$) taken from the same test setup but without the resonator. The calibration formula applied for the (S_{21}) parameter is given by

$$\Delta S_{21} = \mathrm{S}_{21,TUT} - \mathrm{S}_{21,ref}. \tag{1}$$

All complex S_{21} values were first constructed by reading the $Re(S_{21})$ and $Im(S_{21})$ components, and the final result is given in decibels (dB) as in

$$|\Delta S_{21}| \text{ (dB)} = 20 \log_{10} |\Delta S_{21}|. \tag{2}$$

Simulation results in Fig. 2 show the reference S_{21}, simulated S_{21} with the tag and the calibrated S_{21}. The resonance frequency of the tag is 3.28 GHz, which can be observed in the calibrated S_{21} plot.

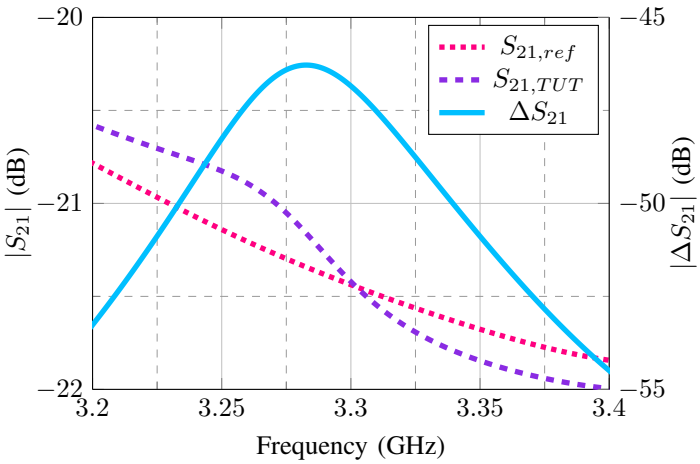

Fig. 2: Simulated reference S_{21} ($S_{21,ref}$), S_{21} with tag ($S_{21,TUT}$), and resulting calibrated S_{21} ($|\Delta S_{21}|$ (dB)) plots.

III. Modelling of the Environmental Effects

For the simulation setup, commercial seedling trays, as illustrated in Fig. 3, are used as the reference structure. Commercially available trays typically measure 30 cm × 50 cm and contain varying numbers of cells. To simplify the modelling process while maintaining geometric representativeness, a 40 cm × 40 cm boundary is set in the simulation environment. Inside this area, pepper plants are modelled as simplified 3D sapling-like structures and uniformly arranged.

Fig. 3: Commercial seedling tray.

For the transmission measurements, two double-ridged horn antennas are employed as transmitter and receiver, each operating over the 2–6 GHz frequency band. The input power level of the transmitter antenna is set to 1 W. The antennas are aligned along the x-axis, separated by 60 cm, and positioned 10 cm from the opposite edges of the tray, as illustrated in Fig. 4. The antennas are polarisation matched, enabling the evaluation of transmission characteristics (S_{21}) across different planting densities.

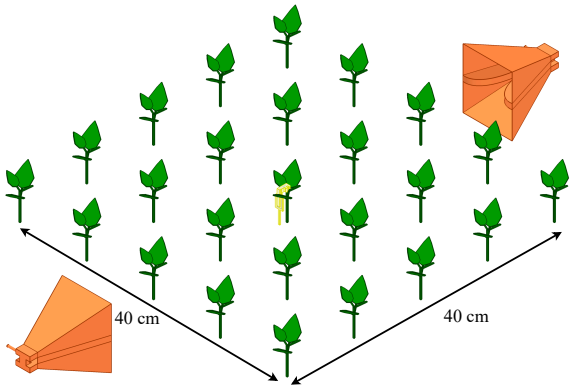

Fig. 4: Full simulation setup with double-ridged horn antennas. The seedling tray boundary is 40 cm × 40 cm. The separation of the horn antennas is 60 cm from each other, and 10 cm from the tray boundary.

In order to analyse different propagation scenarios, first, the planting density is changed. 5×5, 7×7, and 9×9 arrays are located in the seedling tray as shown in Fig. 5. These array configurations correspond to different planting densities within the same physical area. Secondly, the dielectric properties of the plants are varied to represent differing water contents of the plants. The relative permittivity (ϵ_r) of the plant material was varied between 30 and 70 in steps of 20. The plant conductivity was fixed at 2 S/m. Furthermore, all plants are assigned identical and homogeneous dielectric properties to ensure consistency.

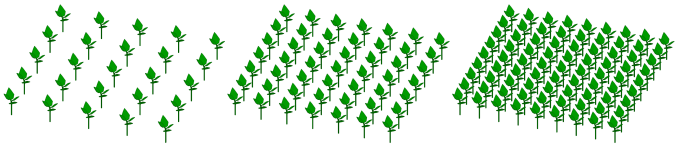

(a) (b) (c)

Fig. 5: Varying planting densities for the simulation setup, (a) 5×5, (b) 7×7, (c) 9×9.

IV. Results and Discussion

The performance of the C-like CRFID tag is quantified by the $|\Delta S_{21}|$ (dB), where a higher peak indicates better readability. Fig. 6(a) shows that the peak value remains relatively constant, changing within a 1 dB range for varying ϵ_r values in the low-density 5×5 configuration. On the other hand, Fig. 6(c) and Fig. 6(e) result in a slight decrease of peak value, as ϵ_r value increases in the 7×7 and 9×9 planting densities. Hence, it can be concluded that the influence of water content is minimal at low densities, but it becomes more pronounced with increasing density.

As planting density increases from 5×5 to 9×9, the peak height drops by nearly 3 dB in Fig. 6(b), indicating a clear inverse relationship between plant density and signal strength. The dense physical arrangement of the plants directly causes this reduction by increasing wave blocking and scattering. This decrease in peak value is even higher at the higher ϵ_r values seen in Fig. 6(d) and Fig. 6(f). The combination of high planting density and high plant water content attenuates the peak value by up to 6 dB.

This attenuation is demonstrated when analysing the best and worst case scenarios; specifically, comparing the 5×5 planting density with $\epsilon_r = 30$ and the 9×9 planting density with $\epsilon_r = 70$ reveals approximately 6 dB decrease in peak value at the operating frequency of the tag, which confirms the effect of both factors on system performance.

To analyse the effect of operating frequency on the sensing performance, three C-like tags are designed with arm lengths (L) of 15 mm, 13 mm, and 11 mm, ensuring their resonance frequencies remain within the Ultra-Wideband (UWB) spectrum. Simulations are done with a setup of a seedling tray with plant density of 7×7 and $\epsilon_r = 50$ and a plant-free setup, only with a C-like tag and horn antennas. The high dielectric loading and scattering caused by the plants result in a downward frequency shift of at least 30 MHz and a minimum peak height reduction of 3 dB for all C-like tags as seen in Fig. 7.

V. Conclusion

This study investigates the readability of a biodegradable C-like Chipless RFID tag designed for plant growth monitoring in varying simulated environmental conditions. Increased planting density and increased ϵ_r value of plants affect the backscatter link, resulting in a reduction in the peak height. It has been observed that as the planting density increases from 5×5 to 9×9, the peak height experiences a decrease of at least 3 dB. The decline in peak height increases as the water content of the plants increases, although the effect of water content is not as significant for a constant planting density. Future works will focus on advanced signal processing techniques such as Short-Time Fourier Transform (STFT) to mitigate the need for calibration and ensure robust, high-resolution performance in harsh agricultural environments.

Acknowledgment

This project is supported by the British Council Research Environments Grant under the reference code RE2023-101.

References

[1] M. N. Mowla, N. Mowla, A. F. M. S. Shah, K. M. Rabie and T. Shongwe, "Internet of Things and Wireless Sensor Networks for Smart Agriculture Applications: A Survey," in IEEE Access, vol. 11, pp. 145813-145852, 2023, doi: 10.1109/ACCESS.2023.3346299.

[2] A. Ahmadihaji, R. Izquierdo and A. Shih, "From Chip-Based to Chipless RFID Sensors: A Review," in IEEE Sensors Journal, vol. 23, no. 11, pp. 11356-11373, 1 June1, 2023, doi: 10.1109/JSEN.2023.3266316.

[3] C. Occhiuzzi et al., "Automatic Monitoring of Fruit Ripening Rooms by UHF RFID Sensor Network and Machine Learning," in IEEE Journal of Radio Frequency Identification, vol. 6, pp. 649-659, 2022, doi: 10.1109/JRFID.2022.3174272.

[4] S. Dey, E. M. Amin and N. C. Karmakar, "Paper Based Chipless RFID Leaf Wetness Detector for Plant Health Monitoring," in IEEE Access, vol. 8, pp. 191986-191996, 2020, doi: 10.1109/ACCESS.2020.3033191.

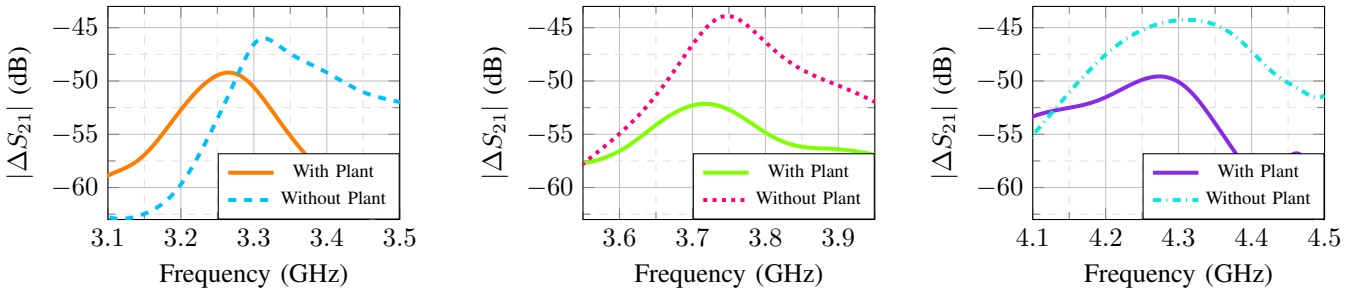

(a) $f_1 = 3.3$ GHz with $L = 15$ mm (b) $f_2 = 3.75$ GHz with $L = 13$ mm (c) $f_3 = 4.3$ GHz with $L = 11$ mm

Fig. 7: $|\Delta S_{21}|$ (dB) plots comparing plant-free and 7×7 plant density with $\epsilon_r = 50$ for three different C-like tags: (a) $f_1 = 3.3$ GHz with $L = 15$ mm, (b) $f_2 = 3.75$ GHz with $L = 13$ mm, and (c) $f_3 = 4.3$ GHz with $L = 11$ mm.

[5] A. Vena, L. Sydänheimo, M. M. Tentzeris and L. Ukkonen, "A Fully Inkjet-Printed Wireless and Chipless Sensor for CO2 and Temperature Detection," in IEEE Sensors Journal, vol. 15, no. 1, pp. 89-99, Jan. 2015, doi: 10.1109/JSEN.2014.2336838.

[6] S. Gopalakrishnan et al., 'A biodegradable chipless sensor for wireless subsoil health monitoring', Sci Rep, vol. 12, no. 1, p. 8011, May 2022, doi: 10.1038/s41598-022-12162-z.

[7] J. Bourely, J. Kim, C. Beyer, O. Vorobyov, X. Aeby, G. Nyström, and D. Briand, "Degradable and printed microstrip line for chipless temperature and humidity sensing," *Advanced Electronic Materials*, vol. 10, no. 10, p. 2400229, 2024, doi: 10.1002/aelm.202400229.

[8] A. Bilir, B. F. Ozcan, Z. C. C. Ozdil and S. Dumanli, "Biodegradable On-plant Resonator for Backscatter Communication Based Wireless Growth Monitoring," 2024 54th European Microwave Conference (EuMC), Paris, France, 2024, pp. 345-348, doi: 10.23919/EuMC61614.2024.10732101.

[9] A. Vena, E. Perret and S. Tedjini, "Chipless RFID Tag Using Hybrid Coding Technique," in IEEE Transactions on Microwave Theory and Techniques, vol. 59, no. 12, pp. 3356-3364, Dec. 2011, doi: 10.1109/TMTT.2011.2171001.

[10] A. Bilir, M. Yavuz, U. O. S. Seker, S. Dumanli, "Wireless In-body Sensing through Genetically Engineered Bacteria," *Nature Communications*,vol. 16, no. 10432, 2025, doi: 10.1038/s41467-025-65416-5.

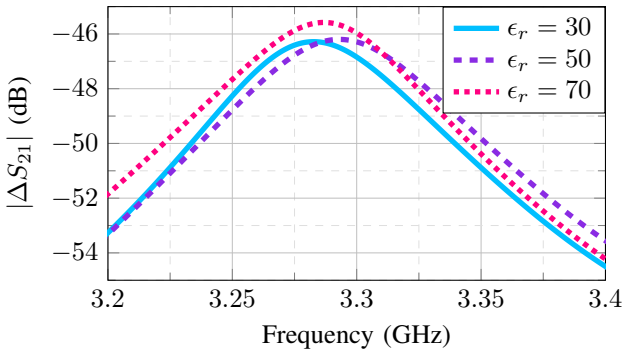

(a) 5×5, $\epsilon_r = 30, 50, 70$

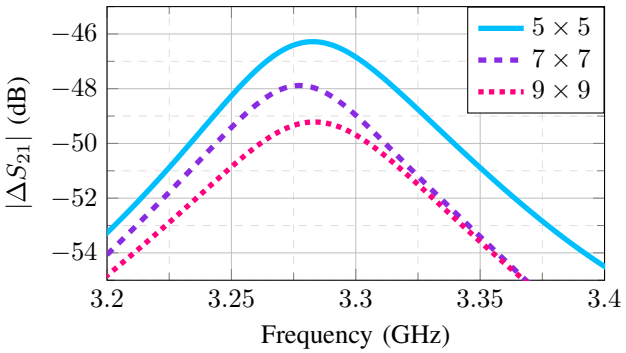

(b) $\epsilon_r = 30$, 5×5, 7×7, 9×9

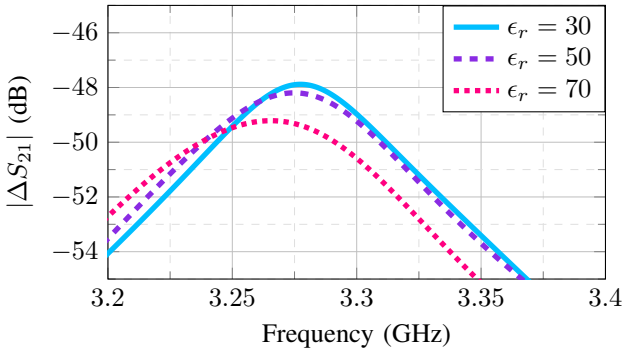

(c) 7×7, $\epsilon_r = 30, 50, 70$

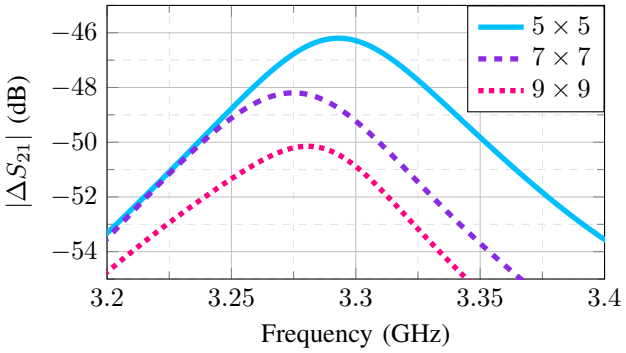

(d) $\epsilon_r = 50$, 5×5, 7×7, 9×9

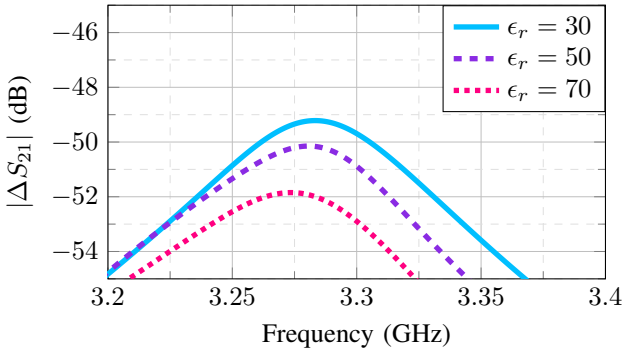

(e) 9×9, $\epsilon_r = 30, 50, 70$

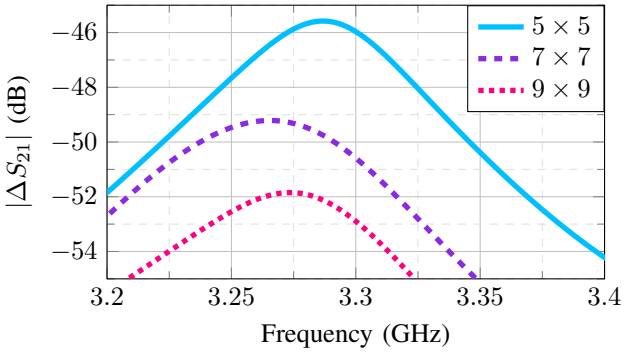

(f) $\epsilon_r = 70$, 5×5, 7×7, 9×9

Fig. 6: $|\Delta S_{21}|$ (dB) plots for (a) plant density of 5×5 while the relative permittivity is varied $\epsilon_r = 30, 50, 70$, (b) relative permittivity of $\epsilon_r = 30$ while the plant density is varied 5×5, 7×7, 9×9, (c) plant density of 7×7 while the relative permittivity is varied $\epsilon_r = 30, 50, 70$, (d) relative permittivity of $\epsilon_r = 50$ while the plant density is varied 5×5, 7×7, 9×9, (e) plant density of 9×9, while the relative permittivity is varied $\epsilon_r = 30, 50, 70$, (f) relative permittivity of $\epsilon_r = 70$ while the plant density is varied 5×5, 7×7, 9×9.